

Monitoring the effects of reduced PS II antenna size on quantum yields of photosystems I and II using the Dual-PAM-100 measuring system

Erhard Pfündel, Christof Klughammer and Ulrich Schreiber

Abstract

The Dual-PAM-100 measuring system is capable of concomitantly recording both absorbance changes and Chl fluorescence. Thus, the instrument permits the simultaneous assessment of energy conversion in PS I and PS II. Here, the Dual-PAM-100 is employed to demonstrate how small PS II antenna size affects both, PS I and PS II photochemistry. By comparing Chl *b*-less barley (*Hordeum vulgare* cv. Donaria mutant chlorina-f2 2800) with wild-type plants, we observed markedly higher PS II photochemical yields, Y(II), in the mutant. The mutant exhibited prominent donor-side limitation of PS I, which entailed decreased photochemical yields of PS I, Y(I). Hence, in the mutant, the high Y(II) values were not paralleled by high values of Y(I), thus resulting in permanent imbalance of PS I and PS II photochemical rates. Therefore, comparable antenna sizes of both photosystems are required for optimal rates of linear electron transport.

Introduction

Photosynthetic production of reducing power requires linear electron flow *via* PS I and II, which implies coordinated rates of charge separation by reaction centers in both photosystems. Because photosynthetic charge separation is driven by absorbed light energy, the proper size of light-harvesting antennae is important for the concerted function of the two photosystems. The light-harvesting complex II (LHC II) represents the main antenna of PS II and it has been proposed that it adjusts the distribution of excitation energy between the two photosystems (Allen 1992, Haldrup *et al.* 2001). Also, LHC II appears to be involved in dissipating excess exciton densities as heat (Demmig-Adams and Adams 1992; Horton and Ruban 1992; Szabó *et al.* 2005).

Chl *b*-less barley leaves lack most LHC II proteins (Bossmann *et al.* 1997), and their total PS II antenna includes only 50 Chl *a* molecules. In comparison, the wild type antenna contains 250 Chl *a* and *b* molecules (Ghirardi *et al.* 1986). Therefore, Chl *b*-less barley leaves have been investigated to examine the consequences of small antenna size for photosynthetic regulation (Andrews *et al.* 1995). Here, we employ parallel measurements of P700 and chlorophyll fluorescence to concomitantly monitor photochemical and non-photochemical quantum yields of PS I and PS II in wild type and Chl *b*-less mutant leaves.

Material and methods

Plants

Two-weeks old plants of the Chl *b*-less mutant *Hordeum vulgare* L. cv. Donaria chlorina-f2 2800, and its wild-type variety, were grown in the laboratory in pots of 12 cm diameter containing commercially available soil

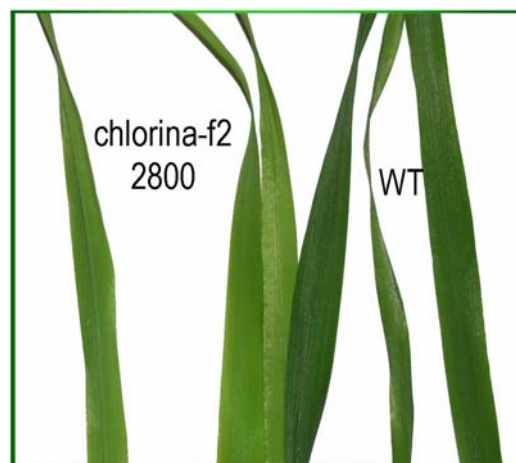


Fig. 1. Wild type (dark green) and mutant (light green) barley leaves.

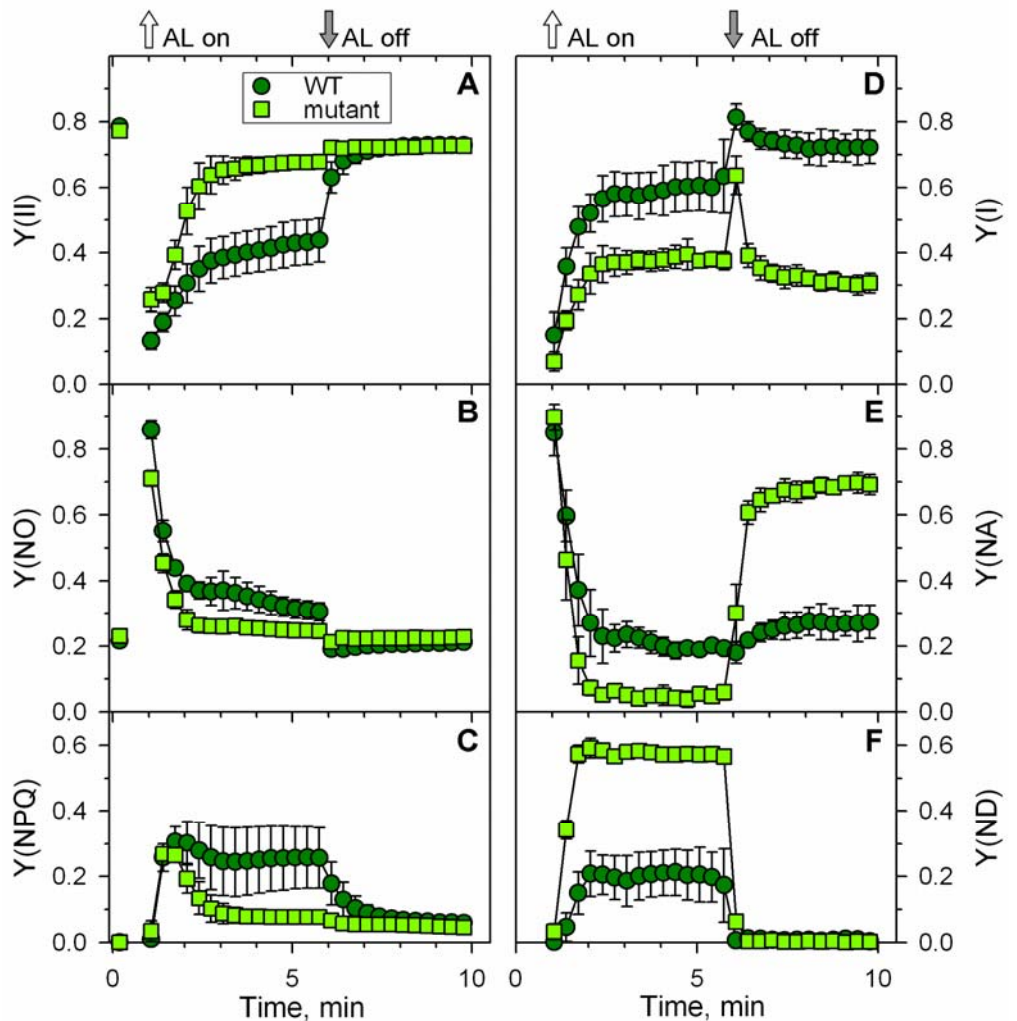
(Kultursubstrat Typ KS II, Terrasan, Rain am Lech, Germany). Plants were watered daily and fertilized weekly using Substral (Scotts Celaflor, Mainz, Germany). Maximum intensities of natural radiation were $50 \mu\text{mol}\cdot\text{m}^{-2}\cdot\text{s}^{-1}$ around noon but reached $500 \mu\text{mol}\cdot\text{m}^{-2}\cdot\text{s}^{-1}$ when plants were directly exposed to the sun during late afternoon hours. Prior to experiments, plants were kept under low light conditions ($3 \mu\text{mol}\cdot\text{m}^{-2}\cdot\text{s}^{-1}$) for at least 1 hour followed by about 3 min darkness.

Instrumentation

All measurements were carried out using a Dual-PAM-100 instrument (Walz, Effeltrich, Germany). Weak modulated measuring light from a 620 nm light emitting diode (LED) and blue actinic light of $250 \mu\text{mol}\cdot\text{m}^{-2}\cdot\text{s}^{-1}$ from 460 nm LED arrays were delivered to the upper leaf surface by a DUAL-DR measuring head. Saturating light pulses of 300 ms duration and $10000 \mu\text{mol}\cdot\text{m}^{-2}\cdot\text{s}^{-1}$

Fig. 2. PS I and PS II regulation during a dark-light-dark transition.

After 1 minute, wild type (WT) and Chl *b*-less barley leaves (mutant) were illuminated with blue actinic light (AL) of 250 $\mu\text{mol}\cdot\text{m}^{-2}\cdot\text{s}^{-1}$ for 5 min. Chl fluorescence and P700 absorbance changes were recorded in parallel. From fluorescence data, the complementary quantum yields of energy conversion in PS II were calculated: A: photochemical energy utilization, $Y(\text{II})$; B: non-regulated energy dissipation, $Y(\text{NO})$; C: regulated (light-activated) energy dissipation $Y(\text{NPQ})$. The corresponding yields in PS I were derived from P700 measurements: D: photochemical energy utilization, $Y(\text{I})$; E: non-photo-chemical energy dissipation due to acceptor side limitation, $Y(\text{NA})$; F: non-photochemical energy dissipation due to donor-side limitation, $Y(\text{ND})$. Data represent mean values of 5 experiments and error bars depict standard deviations.



intensity from 620 nm LED arrays were given simultaneously to the upper and lower leaf side by the DUAL-DR and a DUAL-E emitter unit, respectively. The oxidation/reduction status of PS I reaction centers was followed by the absorbance change at 830 nm (Schreiber *et al.* 1988). For this purpose, 830 nm sample and 875 nm reference beams, both emitted by the DUAL-E unit, were passed through the leaf and received by a photodiode situated in the DUAL-DR measuring head. Both, the DUAL-DR and the DUAL E units were brought into line using a leaf holder (DUAL-B, Walz) in which Perspex rods guided light between the leaf and measuring units.

Measurement of PS I and PS II yields

Experiments were carried out by using the automated Induction and Recovery Curve routine provided by the DualPAM software, with repetitive application of saturation pulses (SP) for assessment of fluorescence and P700 parameters, from which the quantum yields of PS I and PS II were derived by the software.

Firstly, using dark-acclimated plants, the F_0 fluorescence was established and subsequently the F_m fluorescence was determined by the Saturation Pulse method (for a review on PAM fluorometry and the Saturation Pulse method, see Schreiber 2004).

Secondly, the maximal P700 signal was determined by application of an SP after far-red preillumination. It is assumed that under donor-side limited conditions (produced by far-red exposure) a SP transiently induces full P700 oxidation. Briefly after the SP the minimal P700 signal is measured when P700 is fully reduced. The difference signal between the fully reduced and oxidized states is denoted by P_m .

In analogy to the established PAM fluorescence analysis, a modified Saturation Pulse method was applied to assess various P700 parameters (compare *PAM Application Notes 1*: 11-14). This method, which was introduced by Klughammer and Schreiber (1994), is part of the DualPAM software package. Notably, this method not only allows to determine the photochemical quantum yield of PS I, but also to differentiate between the complementary quantum yields caused by energy dissipation by heat emission due to donor- and acceptor-side limitations (see below).

Thirdly, actinic illumination was started and SP were given every 20 s, with the same pulses serving for fluorescence and P700 analysis. Each SP was followed by a 1 s dark-period to determine the minimal P700 signal level P_0 (P700 fully reduced). The fluorescence levels F and F_m' were recorded just before and during each SP,

respectively. The F_o' levels were approximated according to Oxborough and Baker (1997). Three complementary quantum yields of energy conversion in PS II were calculated (Kramer et al. 2004):

Y(II) effective photochemical quantum yield of PS II,

Y(NPQ) quantum yield of light-induced non-photochemical fluorescence quenching, and

Y(NO) quantum yield of non-light-induced non-photochemical fluorescence quenching.

These quantum yields are complementary, i.e. add up to one: $Y(II)+Y(NPQ)+Y(NO)=1$

The P700 signal (P) was recorded just before a SP then briefly after onset of a SP ($P_{m'}$), when maximum P700 oxidation under the effective experimental conditions is observed, and finally at the end of the 1 s dark interval following each SP (P_o determination). The signals P and $P_{m'}$ are referenced against P_o . In this way, unavoidable signal drifts, e.g. due to changes in the water status, do not disturb the actual measurements of P700 parameters.

Three types of complementary quantum yields of energy conversion in PS I were calculated:

Y(I) Effective photochemical quantum yield:

$$Y(I) = (P_{m'} - P) / P_m$$

Y(ND) Quantum yield of non-photochemical energy dissipation in reaction centers which are limited due to a shortage of electrons (donor side limitation)

$$Y(ND) = (P - P_o) / P_m$$

Y(NA) Quantum yield of non-photochemical energy dissipation of reaction centers which are limited due to shortage of electron acceptors (acceptor side limitation):

$$Y(NA) = (P_m - P_{m'}) / P_m$$

As for PSII, these three quantum yields are complementary, i.e. they add up to one:

$$Y(I)+Y(ND)+Y(NA)=1.$$

Results and discussion

Immediately after onset of actinic illumination, the Y(II) values of wild type and mutant leaves dropped from 0.8 to 0.1 and 0.25, respectively (Fig. 2A). At the end of the exposure interval, the Y(II) in wild type leaves approached values of 0.4 whereas the mutant showed values close to 0.7.

The lower Y(II) values in the wild type are primarily due to stronger regulated non-photochemical energy dissipation, as reflected by the higher Y(NPQ) values. Only at the start of illumination, when a full trans-thylakoid ΔpH is not yet established, the higher Y(NO) (caused by higher fraction of closed PS II centers) is responsible for

decreased Y(II) (Fig. 2B). Subsequently, the variations in the ΔpH -dependent Y(NPQ) (Fig. 2C) dominates the pattern of Y(II).

Evidently, in the presence of normal PS II antennae in wild type leaves, light is efficiently harvested so that part of the absorbed light energy is in excess. In this case, regulated non-photochemical dissipation of energy prevents possible damage. In the mutant, which is characterized by small PS II antennae, non-photochemical energy dissipation was considerably smaller. This is particularly true for regulated dissipation, as indicated by Y(NPQ).

It may be noted that Y(NPQ) as well as Y(II), which are primarily affected by regulation, display a distinctly higher variability than Y(NO). Possibly, the variations in regulated states arise from different acclimation states of the LHC II which are formed in response to subtle differences in samples and pre-treatment conditions. Both, the Y(NPQ) and the Y(II), showed much higher variability in wild type than in mutant leaves. Almost certainly, the absence of the LHC II in the mutant reduces the potential to acclimate antenna function to different light exposures and, thus, may explain the low variability of fluorescence data. In contrast to PS II, the photochemical yield of PS I, Y(I), was higher in wild type than in mutant leaves (Fig. 2D).

The low Y(I) in mutant leaves arise from marked donor side limitation of PS I, as reflected by Y(ND), which was threefold higher in mutant than that in wild type leaves (Fig. 2F). The elevated Y(ND) was accompanied by low Y(NA), whereas the Y(ND) and Y(NA) were balanced in wild type leaves (Fig. 2E and F).

Donor-side limitation of PS I in the mutant is consistent with inefficient light absorption by the small PS II antennae of PS II, which provides the electrons by water splitting. Inefficient absorption causes low rates of PS II charge separation that apparently do not match the capacity of PS I. To summarize, small PS II antenna size can efficiently restrict PS I photochemistry via donor side limitation.

The data presented in Fig. 2 reveal another distinct difference between mutant and wild type, which relates to the reactions upon transition from the light to the dark state. In the mutant, strong acceptor-side limitation develops within the first minute following light-off, as reflected by high Y(NA) values (about 0.7 as compared to 0.3 in the wild type). It may be speculated that these high Y(NA) values in the mutant reflect a smaller pool size of PS I acceptors, which may be explained as an adaptation to the donor-side limitation of PS I during illumination.

Conclusion

The P700 & Fluorescence Measuring System Dual-PAM-100 is capable of detecting imbalanced rates of photochemistry of PS I and PS II with high accuracy by simultaneously recording quantum yields of both photo-systems. By using this instrument, we describe donor side limitations of PS I photochemistry caused by small PS II antenna size. In general, however, the method is applicable to and capable of the characterization of all types of factors affecting the interplay between photo-systems such as long-term acclimation of photosynthesis or mutation of photosynthetic components.

References

- Allen IF (1992) Protein phosphorylation in regulation of photosynthesis. *Biochim Biophys Acta* 1098:275-335
- Andrews JR, Fryer MJ, Baker NR (1995) Consequences of LHC II deficiency for photosynthetic regulation in chlorina mutants of barley. *Photosynth Res* 44: 81-91
- Bossmann B, Knoetzel J, Jansson S (1997) Screening of chlorina mutants of barley (*Hordeum vulgare* L.) with antibodies against light-harvesting proteins of PS I and PS II: absence of specific antenna proteins. *Photosynth Res* 52: 127-136
- Demmig-Adams B, Adams WW (1992) Photoprotection and other responses of plants to high light stress. *Annu Rev Plant Physiol Plant Mol Bio* 43: 599-626
- Genty B, Briantais J-M, Baker NR (1989) The relationship between the quantum yield of photosynthetic electron transport and quenching of chlorophyll fluorescence. *Biochim Biophys Acta* 990: 87-92
- Ghirardi ML, McCauley SW, Melis A (1986) Photochemical apparatus organization in the thylakoid membrane of *Hordeum vulgare* wild type and chlorophyll b-less chlorina f2 mutant. *Biochim Biophys Acta* 851: 331-339
- Haldrup A, Jensen PE, Lunde C, Scheller HV (2001) Balance of power: a view of the mechanism of photosynthetic state transitions *Trends Plant Sci* 6: 301-3055
- Horton P, Ruban AV (1992) Regulation of Photosystem II. *Photosynth Res* 34: 375-385
- Klughammer C, Schreiber U (1994) An improved method, using saturating light pulses, for the determination of photosystem I quantum yield via P700⁺-absorbance changes at 830 nm. *Planta* 192: 261-268
- Kramer DM, Johnson G, Kiirats O, Edwards GE (2004) New fluorescence parameters for the determination of Q_A redox state and excitation energy fluxes. *Photosynth Res* 79: 209-218
- Oxborough K, Baker NR (1997) Resolving chlorophyll a fluorescence images of photosynthetic efficiency into photochemical and non-photochemical components – calculation of q_P and F_v/F_M without measuring F₀. *Photosynth Res* 54: 135-142
- Schreiber U (2004) Pulse-Amplitude (PAM) fluorometry and saturation pulse method. In: Papageorgiou G, Govindjee (eds) *Chlorophyll fluorescence: A signature of Photosynthesis*. Kluwer Academic Publishers, Dordrecht, The Netherlands. pp 279-319
- Schreiber U, Klughammer C, Neubauer C (1988) Measuring P700 absorbance changes around 830 nm with a new type of pulse modulation system. *Z Naturforsch* 43c: 686-698
- Szabó I, Bergantino E, Giacometti GM (2005) Light and oxygenic photosynthesis: energy dissipation as a protection mechanism against photo-oxidation. *EMBO Rep* 6: 629-634